Thermal Properties of Ionic Liquids and IoNanofluids of Imidazolium and Pyrrolidinium Liquids†

C. A. Nieto de Castro,* M. J. V. Lourenço, A. P. C. Ribeiro, E. Langa, and S. I. C. Vieira

Centro de Ciências Moleculares e Materiais and Departamento de Química e Bioquímica, Faculdade de Ciências da Universidade de Lisboa, Campo Grande, 1749-016 Lisboa, Portugal

P. Goodrich and C. Hardacre

The QUILL Centre/School of Chemistry and Chemical Engineering, Queen's University Belfast, Belfast BT9 5AG, U.K.

Complex systems based on nanomaterials and common solvents have been shown to have thermophysical properties that can revolutionize current utilization of heat transfer fluids and heat storage cycles. This has been made possible by the existence of thermal conductivity enhancements derived from the presence of additional mechanisms of heat transfer in comparison with the base solvent. Ionic liquids have been shown to have thermophysical properties that justify the replacement of several of the chemical processes now under exploitation, and some of the solvents used, because they can in certain conditions, be considered as green solvents. Dissolving (or mixing as a thermally stable suspension) nanoparticles in ionic liquids, forms "bucky gels", or IoNanoFluids, which we have recently shown to have thermal conductivity enhancements ranging from (5 to 35) %. This paper reports data on the thermal conductivity of the ionic liquids 1-hexyl-3-methylimidazolium tetrafluoroborate (CAS Number, 244193-50-8), [C_6mim][BF_4], 1-butyl-3-methylimidazolium hexafluorophosphate (CAS Number, 174501-64-5), [C_4mim][PF_6], 1-hexyl-3-methylimidazolium hexafluorophosphate (CAS Number, 304680-35-1), [C_6mim][PF_6], 1-butyl-3-methylimidazolium trifluoromethanesulfonate (CAS Number, 174899-66-2), [C_4mim][CF_3SO_3], and 1-butyl-1-methylpyrrolidinium bis{(trifluoromethyl)sulfonyl}imide (CAS Number, 223437-11-4), [C_4mpyrr][$(CF_3SO_2)_2$N], and IoNanofluids with multiwalled carbon nanotubes (MWCNTs) as a function of temperature and discuss the molecular theories of heat transfer and storage in these types of systems. Moderate thermal conductivity enhancements, between (2 and 9) %, were found for the systems studied, showing a week dependence on temperature. It also reports heat capacity values for [C_4mim][BF_4] and [C_4mim][PF_6]. Values of the heat capacity of an IoNanofluid, C_4mim][PF_6] with (1 and 1.5) % Baytubes, are reported for the first time, showing also an enhancement (8 %), a fact that deserves further investigation in a near future. The behavior of these nanofluids, along with that of ionic liquids of the type studied, suggests that nanocluster formation and preferred paths for heat transfer and storage are present and are likely to be the cause of the phenomena found. However, existing theories cannot yet explain the results obtained.

1. Introduction

The current situation of the world economy requires the search for alternative energies to conventional fuels, the optimization of current energy technologies, and the search for new and clean working fluids in order to decrease the energy consumption without destroying the developmental needs of different countries. In the field of heat transfer, all current liquid coolants used at low and moderate temperatures exhibit extremely poor thermal conductivity and heat storage capacities, as the classical equipment for heat transfer uses working fluids that were developed, tested, and applied in a world of positive economical growth. In contrast, the uses of these chemical technologies today are considered unsustainable. Although increased heat transfer can be achieved creating turbulence, increasing surface area, and so forth, ultimately the transfer will still be limited by the small thermal conductivity of the fluid. Therefore, there is a need for new heat transfer liquids with the challenge being to design more efficient liquids in terms of energy conversion for domestic and industrial applications.

The screening of all possibilities leads us to the use of nanofluids, recently reviewed by Murshed et al.[1] Using the fact that solid materials, namely metals or carbon nanotubes (CNTs), have a thermal conductivity at room temperature several orders of magnitude higher than fluids, it has been shown that the thermal conductivity of fluids containing suspended particles (metallic, nonmetallic) could be significantly higher than the base fluids. Applying nanotechnology to heat transfer, Choi et al.[2] invented the term nanofluid to designate a new class of heat transfer fluids formed by the dispersion of nanometer-sized solid particles, rods, or tubes in traditional heat transfer fluids. From the investigations performed thereafter, nanofluids were found to have higher thermal conductivity than those of the base fluids.[1] The suspensions/emulsions are stable and Newtonian, and these nanofluids have been proposed as 21st century heat transfer agents for cooling devices that respond more efficiently to the challenges of great heat loads, higher power engines and brighter optical devices, increased transportation, micromechan-

† Part of the "2009 Iberian Conference on Ionic Liquids".

* To whom correspondence should be addressed. E-mail: cacastro@fc.ul.pt.

10.1021/je900648p CCC: $40.75
Published on Web 11/13/2009

ics, instrumentation, HVAC (heating, ventilating, and air-conditioning), and medical applications.[1,3,4] Some consider them already to be the cooling media of the future.[5] Although significant progress has been made, variability in the heat transfer characteristics is present that may be the result of the synthesis of the nanofluids being quite delicate. In fact, a nanofluid does not mean necessarily a simple mixture of solid particles and a liquid in the thermodynamic definition, and the techniques used by different authors are sometimes ill-defined,[1,5] as discussed below.

Previous studies in nanofluids have used common liquids such as water, ethylene glycol, or oils. No innovation has been performed so far in the base fluids until the publication by Ribeiro et al.[6] In this paper, we report the first results for the thermal conductivity of ionic liquids with CNTs for alkylmethylimidazolium liquids. Ionic liquids are fluids currently under intense study for chemical and materials processing, as environmentally friendly solvents and reaction fluids ("green" solvents).[7−9] These materials are generally are nonflammable and nonvolatile under ambient conditions and their thermophysical properties, being compatible with the requisites of heat transfer fluids, can be fine-tuned by their structure and tailored to satisfy the specific application requirements. According to the American National Renewable Energy Laboratory, there have been no major developments in the field of thermal energy storage systems in the 1990s and the discovery of ionic liquids systems qualifies them as a viable thermal fluid, a fact that is supported by recent applications as thermal fluids.[10,11]

The discovery that carbon nanotubes and room-temperature ionic liquids can be blended to form gels that may be used to make novel electronic devices, coating materials, and antistatic materials, opens a completely new field.[12,13] "Bucky gels" are blends or emulsions of ionic liquids with nanomaterials, mostly nanocarbons (tubes, fullerenes, spheres). The possibility of using ionic liquids containing dispersed nanoparticles with specific functionalization, for example, single-walled nanotubes (SWCNTs), multiwalled nanotubes (MWCNTs) and fullerenes (C60, C80, etc.), opens the door to many applications. The use of nanoparticles as heat transfer enhancers allows us to associate small quantities of different types of nanomaterials to ionic liquids, IoNanofluids, which are highly flexible such that they can be designed (target-oriented) in terms of molecular structure to achieve the desired properties necessary to accomplish a given job. This is possibly due to the complex interactions ionic liquids, nanomaterials in the complex emulsions they form, as discussed below.

This paper reports thermal conductivity measurements of $[C_6mim][BF_4]$, $[C_4mim][PF_6]$, $[C_6mim][PF_6]$, $[C_4mim][CF_3SO_3]$, and $[C_4mpyrr][(CF_3SO_2)_2N]$ at temperatures between 293 and 363 K and of the corresponding IoNanofluids composed of 0.01 mass fraction MWCNTs in the ionic liquids, as a function of temperature. It also reports on the heat capacity of the IoNanofluid, $[C_4mim][PF_6]$, with two MWCNT mass fractions of 0.01 and 0.015, as a function of temperature. The molecular theories on heat transfer in nanofluids applied to our systems are also discussed.

2. Experimental Section

All ionic liquids were synthesized and purified at the QUILL Centre, Belfast, according to procedures found elsewhere.[14,15] They were prepared via metathesis reactions from the appropriate $[C_n mim]Cl$. Samples were extensively washed using distilled water and dried while stirring overnight at 70 °C under high vacuum (0.1 Pa) prior to use. All ionic liquids were analyzed by ^1H and ^{13}C NMR and elemental analysis and showed excellent agreement with the reported data. The water content was measured using Coulometric Karl Fischer titration (Metrohm 831) before and after each thermal conductivity measurement. In all cases, the water mass fraction was found to be less than 0.0002. The halide content of ionic liquids was determined using suppressed ion chromatography[16] and all ionic liquids had a chloride mass fraction less than $5 \cdot 10^{-6}$, unless otherwise stated.

Table 1. Baytubes Product Specification[a]

property	value	unit	method
C-purity	> 0.99	mass fraction	elementary analysis
free amorphous carbon	not detectable	%	TEM
number of walls	3 to 15		TEM
outer mean diameter	13 to 16	nm	TEM
outer diameter distribution	5 to 20	nm	TEM
inner mean diameter	4	nm	TEM
inner diameter distribution	2 to 6	nm	TEM
length	1 to 10	mm	SEM
bulk density	140 to 230	$kg \cdot m^{-3}$	EN ISO 60

[a] http://www.baytubes.com/product_production/baytubes_data.html.

The carbon nanotubes used were Multiwalled Carbon Nanotubes Baytubes C150 HP from Bayer Material Science, a development product. Specifications can be found in Table 1. Baytubes are produced in a high-yielding catalytic process based on chemical vapor deposition. The process yields easy to handle agglomerates with high apparent density. The optimized process results in a high degree of purity (low concentration of residual catalyst and absence of free amorphous carbon). Baytubes are agglomerates of multiwall carbon nanotubes with low outer diameter, a narrow diameter distribution, and an ultrahigh aspect ratio (length-to-diameter ratio). They show excellent tensile strength and E-modulus, as well as exceptional thermal and electrical conductivity.

As explained above, the synthesis of the nanofluids is quite delicate. There are two main techniques used with normal solvents, the two-step process and the direct evaporation technique or single step. Most researchers use the two-step process by dispersing commercial or self-produced nanoparticles in the liquid, a technique that can create large particle agglomerates, destroyed by adding surfactants or using dispersion techniques. Aida and co-workers found that imidazolium-ion-based ionic liquids were excellent dispersants for CNTs,[12,13] forming physical gels, that could be reproduced using sonification or grinding the suspension in an agate mortar with a pestle. These techniques were followed in present work to obtain very stable emulsions, with mass fractions of 0.01 and 0.015 loading of MWCNTs (Sonicator Sonics & Materials, model VC50).

Thermal conductivity data were measured using a KD2 Pro Thermal Properties Analyzer (Labcell Ltd., UK). The principle of measurement is based on the transient hot-wire method, and an electrically isolated probe coated with a thin coating of an insulator was used, as the ionic liquid is electrically conducting.[8,17,18] The meter consists of a thermal probe (1.3 mm diameter, 60 mm length), containing a heating element and a thermoresistor, which should be inserted into the sample vertically, rather than horizontally, to minimize the possibility of inducing convection. The measurement is made by heating the probe within the sample while simultaneously monitoring the temperature change of the probe. A microprocessor, connected to the probe, is used to control the heating rate, measure the temperature change data, and calculate the thermal conductivity based on a parameter-

Table 2. Reference Materials Used for the Temperature Calibration

reference material	origin	mass fraction purity	T_{fus} / K	$\Delta_{fus}H_m$ / J·mol^{-1}	reference
Hg	BDH	> 0.99999	234.29 ± 0.01	2295.3 ± 0.8	46
Ga	Alfa Chemicals	0.999999	302.9146	5569 ± 50	47
			302.92 ± 0.02	5590 ± 40	48
In	LGC 2601	0.99999	429.76 ± 0.02	3296 ± 9	CRMC[a]
Sn	LGC 2609	0.9999998	505.07 ± 0.02	7187 ± 4	CRMC[a]
Pb	LGC 2608	0.99996	600.62 ± 0.02	4756 ± 11	CRMC[a]
Zn	LGC 2611	0.99996	692.68 ± 0.02	7103 ± 31	CRMC[a]

[a] CRMC - Certified reference materials certificate - LGC (U.K.).

Table 3. Comparison between the Temperature and Enthalpy of Fusion of Mercury[a], Gallium, Indium (LGC 2601), and Tin (LGC 2609)

	Hg	Ga	In	Sn
$(\Delta_{fus}H)_{std}$/J·mol^{-1}	2295.3 ± 0.8[46,48]	5569 ± 60[46]	3296 ± 9	7187 ± 4
		5590 ± 40[48]		
$(\Delta_{fus}H)_{exp}$/J·mol^{-1}	2268 ± 33	5568 ± 71	3249 ± 35	7083 ± 74
T_{std} /K	234.29 ± 0.01[46,47]	302.92 ± 0.02[48]	429.76 ± 0.02	505.07 ± 0.02
		302.9146[47]		
T_{exp} /K	233.58 ± 0.19[c]		429.68 ± 0.07	505.01 ± 0.07
		303.08 ± 0.29[b]	429.66 ± 0.02[b]	505.16 ± 0.15[b]

[a] p.a., Bidistilled. [b] Extrapolation to zero scanning rate. [c] At 2 K·min^{-1}.

corrected version of the temperature model given by Carslaw and Jaeger[19] for an infinite line heat source with constant heat output and zero mass in an infinite medium. For this model to accurately describe the physical behavior of a system, the heat source must closely approximate an infinitely long, thin line. Kuitenberg et al.[20] describe the solutions for a heated cylindrical source with a non-negligible radius and finite length which is used for this probe. Both models give equally good fit to the temperature data but differ slightly in value for the fitting parameters, and these differences can be accounted for by the calibration, allowing the former, simpler model to be used, which has been employed herein.[18] Before and after analysis of the ionic liquid samples, the meter was calibrated using water and a standard sample of glycerol of known thermal conductivity. Approximately 15 cm^3 of the sample to be analyzed was sealed in a glass sample vial. The probe was inserted vertically into the sample via a purpose-made port in the lid of the vial. The sealed vial was then fully immersed in a temperature-controlled water bath (Grant GD120) and allowed to equilibrate at the desired temperature. Once the sample reached the required temperature, a further 15 min was allowed to pass before carrying out the measurement to ensure complete equilibration. At least four measurements were taken at each temperature with a delay of at least 15 min between each measurement, to ensure reproducibility. More details can be found in the work of Ge et al.[21] The uncertainty of the thermal conductivity was estimated from the standard deviations of experimental and calibration measurements to be ± 0.005 Wm^{1-}·K^{-1}. The uncertainty of the temperature is estimated to be ± 1 K.

Heat capacity measurements were measured with a differential scanning calorimeter (DSC-111, Setaram, France), which was calibrated in enthalpy (Joule effect) and temperature (CRMs, LGC, UK).[22,23] The melting temperatures of Hg, Ga, In, Sn, Pb, and Zn were used to calibrate the temperature indicated by the instrument and the heat of fusion of these metals was used to assess the calibration uncertainty due to the Joule effect. Table 2 shows the reference materials used, their origin and purity, as well as the recommended values for the enthalpies and temperatures of fusion. Table 3 show the results obtained for the melting (fusion) temperatures and fusion enthalpies of the Hg, Ga, In, and Sn. The uncertainty in the enthalpy measurements was found to be of the order of 1 %, while the temperature measurements agree within 0.1 K with the standard values, except for mercury, where data only at 2 K min^{-1} was determined.

The heat capacity was obtained using closed stainless steel crucibles, by continuous method-standard zone, with a scanning rate of 2 K min^{-1} (Setaram SETSOFT 2000, Version 3.0). The mass of the samples was confirmed after each run to confirm possible weight losses. The heat capacity was obtained from the total energy detected by the calorimeter, $(Q_P)_{meas}$, the calibration constant, K, and the scanning rate β using eq 1

$$C_p = \frac{(Q_P)_{meas}}{K \cdot \beta} \quad (1)$$

The measurement technique uses a double experiment performing two nearly identical runs, one with the two cells without sample and the other with the sample in one of the cells. In this way, any differences between the two crucibles are eliminated from the final signal to be used in eq 1. The uncertainty of the heat capacity determinations is better than 1.5 % at a 95 % confidence level (The ISO definition, with a coverage factor $k = 2$ is used. To obtain the value for the accuracy it must be divided by 2).[24] We have checked the accuracy of the measurements by measuring the heat capacity of certified reference material sapphire (NIST SRM-707), between room temperature and 430 K, and found deviations less than 1.5 %, with an average absolute deviation (AAD) of 0.68 %.

3. Results and Discussion

3.1. Thermal Conductivity of Ionic Liquids. The thermal conductivity of [C_6mim][BF_4], [C_4mim][PF_6], [C_6mim][PF_6], [C_4mim][CF_3SO_3], and [C_4mpyrr][$(CF_3SO_2)_2$N] were measured between 293 and 353 K at 0.1 MPa. Thermal conductivities for [C_2mim][$(CF_3SO_2)_2$N], [C_4mim][$(CF_3SO_2)_2$N], [C_6mim][$(CF_3SO_2)_2$N], [C_8mim][$(CF_3SO_2)_2$N], and [C_4mim][BF_4] have also been reported in ref 6 Figure 1 and Table 4 shows the results obtained. It can be seen that the variation is linear and that no data point departs from linearity by more than ± 0.6 %. Table 5 shows the coefficients of regression for eq 2 and the root-

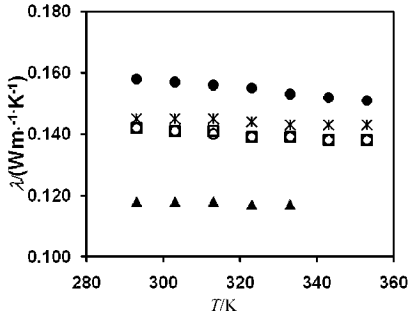

Figure 1. Thermal conductivity λ of ionic liquids as a function of temperature T. ●, [C_6mim][BF_4]; ○, [C_4mim][CF_3SO_3]; ▲, [C_4mpyrr][$(CF_3SO_2)_2$N]; ∗, [C_4mim][PF_6]; □, [C_6mim][PF_6].

Table 4. Thermal Conductivity of Ionic Liquids As a Function of Temperature

	λ/W·m^{-1}·K^{-1}				
T/K	[C_6mim][BF_4]	[C_4mim][CF_3SO_3]	[C_4mpyrr][$(CF_3SO_2)_2$N]	[C_4mim][PF_6]	[C_6mim][PF_6]
293	0.158	0.142	0.118	0.145	0.142
303	0.157	0.141	0.118	0.145	0.141
313	0.156	0.140	0.118	0.145	0.141
323	0.155	0.139	0.117	0.144	0.139
333	0.153	0.139	0.117	0.143	0.139
343	0.152	0.138		0.143	0.138
353	0.151	0.138		0.143	0.138

mean-square deviations of the fits. The variance of the fits do not exceed 0.48 mW·m^{-1}·K^{-1}, about 0.3 %.

$$\lambda(\mathrm{W \cdot m^{-1} \cdot K^{-1}}) = a_1 + a_2(T/\mathrm{K}) \quad (2)$$

Few other studies have been reported. Tomida et al.[25] measured the thermal conductivity of [C_4mim][PF_6], and [C_6mim][PF_6] from 294 to 335 K at pressures up to 20 MPa, using the transient short-hot-wire method with an uncertainty of (2 to 4) %. Their samples were synthesized, dried by heating in a vacuum, and purified by adsorbing the impurities onto activated charcoal. Therein, the water content after the measurements was found to be in the range (70 to 90) ppm. Ge et al.[21] reported measurements for [C_4mpyrr][$(CF_3SO_2)_2$N] and [C_4mim][CF_3SO_3] using the same instrument presented in this work with an estimated uncertainty of ± 0.005 W·m^{-1}·K^{-1}. The water content was found to be less than 80 ppm, and the chloride mass fraction was less than $5 \cdot 10^{-6}$. Figure 2 shows the deviations of our data from eq 2 and it can be seen that no data point deviated from the linear fitting by more than 0.5 %.

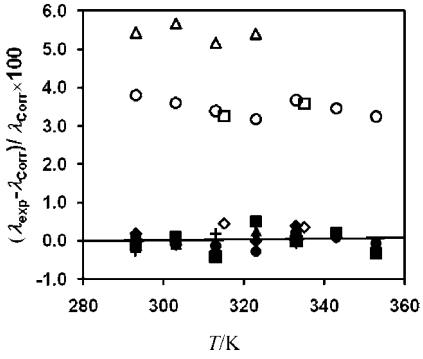

Figure 2. Deviations of the thermal conductivity reported in this paper λ along with results from other workers from eq 2, as a function of temperature T. ●, [C_6mim][BF_4]; +, [C_4mim][CF_3SO_3]; ▲, [C_4mpyrr][$(CF_3SO_2)_2$N]; ◆, [C_4mim][PF_6]; ■, [C_6mim][PF_6]; △, C_4mpyrr][$(CF_3SO_2)_2$N], Ge at al. (2007);[21] ○, [C_4mim][CF_3SO_3], Ge at al. (2007);[21] ◇, [C_4mim][PF_6], Tomida et al. (2007);[25] □, [C_6mim][PF_6], Tomida et al. (2007).[25]

In addition, the deviations from our fits of the data from Ge et al.[21] for [C_4mpyrr][$(CF_3SO_2)_2$N] and [C_4mim][CF_3SO_3] and by Tomida et al.[25] for [C_4mim][PF_6], and [C_6mim][PF_6] were obtained using a bare platinum wire. In all cases, the data agree within the error associated with the methods used. For both the data of Tomida et al.[25] and Ge et al.,[21] the previously reported data is systematically slightly higher than those reported in this study, which may be associated with higher purity samples utilized in the present study. Ge et al.[21] showed that small levels of water or halide, which are common impurities from the synthesis of ionic liquids, both increase the thermal conductivity of ionic liquids.

3.2. Heat Capacity of Ionic Liquids. Measurements of the heat capacity of [C_4mim][BF_4] and [C_4mim][PF_6] were obtained at a pressure of 0.1 MPa at temperatures between 308 and 423 K and Table 6 shows the results obtained. The experimental values were fitted as a function of temperature with the polynomial given by eq 3

$$C_p(\mathrm{J \cdot mol^{-1} \cdot K^{-1}}) = b_1 + b_2(T/\mathrm{K}) + b_3(T/\mathrm{K})^2 \quad (3)$$

Table 7 shows the coefficients of regression for eq 3 and the root-mean-square deviations associated with the fits for [C_4mim][BF_4]. The variance is 0.914 J·mol^{-1}·K^{-1}, approximately 0.3 %. Figure 3 shows the variation of heat capacity with temperature, together with the results obtained by different authors. Data have been reported by Rebelo et al.,[26] Kim et al.,[27] Fredlake et al.,[28] Waliszewski et al.,[29] Van Valkenburg et al.,[30] and Garcia-Miaja et al.[31,32] All these data were obtained with DSC. A wide variation between the data sets of up to 20 % at room temperature is observed. This situation is very uncommon in calorimetry; however it is known that, apart from differences in sample purity, the DSC used must be well calibrated and this may explain the scatter of data. Figure 4 shows the deviations between our data and other data. It should be noted that results with deviations greater than ± 2 % are not included. Our data agrees with the data from Rebelo et al.,[26] between (0.9 and 2.5) %, Waliszewski et al.,[29] between (0.86 and 2) %, Van Valkenburg et al.,[30] between (1 and 2) %, and Garcia-Miaja et al.,[32] to within 0.7 %. The data reported by Fredlake et al.[28] deviates by more than −3 %, while that of Kim et al.[27] deviates between (8 and 12) %. All these numbers are well within the mutual uncertainty of the data, except those of Kim et al.[27]

Table 7 also shows the coefficients of regression for eq 3 and the root-mean-square deviations of the fits for [C_4mim][PF_6]. The variance is 1.29 J·mol^{-1}·K^{-1}, approximately 0.3 %. Figure 5 shows the variation of heat capacity with temperature, together with the results obtained by different authors. Data for this liquid has been reported by Holbrey et al.,[33] Kabo et al.,[34] Fredlake et al.,[28] and Troncoso et al.[35] With the exception of the data reported by Kabo et al.,[34] which were obtained using a heat bridge calorimeter, all the remaining data were obtained by DSC. Figure 4 also shows the deviations between our data and other data for [C_4mim][PF_6]. Again results with deviations greater than ± 2 % are not included. Our data agrees with the data of Troncoso et al.[35] between (0.4 and 0.6) % and with Kabo et al.[34] between (0.8 and 1.2) %. These variations are within the expected uncertainty of the data with in all cases, the data reported herein being slightly lower. In contrast, the data reported by Fredlake et al.[28] and especially those reported by Holbrey et al.[33] are much lower than our data with the latter data showing deviations of up to − 20 %.

Table 5. Coefficients of Equation 2 for Pure Ionic Liquids and IoNanofluids (1 wt % MWCNT)

	$a_1 \pm \sigma_{a1}$ / W·m^{-1}·K^{-1}	$10^4(a_2 \pm \sigma_{a2})$ / W·m^{-1}·K^{-2}	σ / W·m^{-1}·K^{-1}
	Ionic Liquid		
[C$_6$mim][BF$_4$]	0.19379 ± 0.00179	−1.214 ± 0.053	0.00029
[C$_4$mim][CF$_3$SO$_3$]	0.16149 ± 0.00248	−0.679 ± 0.077	0.00041
[C$_4$mpyrr][(CF$_3$SO$_2$)$_2$N]	0.12699 ± 0.00313	−0.300 ± 0.100	0.00032
[C$_4$mim][PF$_6$]	0.15784 ± 0.00253	−0.429 ± 0.078	0.00041
[C$_6$mim][PF$_6$]	0.16279 ± 0.00292	−0.714 ± 0.090	0.00048
	IoNanofluid		
[C$_6$mim][BF$_4$] + MWCNT	0.17631 ± 0.00179	−0.357 ± 0.006	0.00029
[C$_4$mim][CF$_3$SO$_3$] + MWCNT	0.16310 ± 0.00200	−0.321 ± 0.006	0.00032
[C$_4$mpyrr][(CF$_3$SO$_2$)$_2$N] + MWCNT	0.13279 ± 0.00313	−0.300 ± 0.010	0.00032
[C$_4$mim][PF$_6$] + MWCNT	0.16501 ± 0.00372	−0.500 ± 0.115	0.00061
[C$_6$mim][PF$_6$] + MWCNT	0.15844 ± 0.00179	−0.500 ± 0.055	0.00029

Table 6. Heat Capacity C_P of [C$_4$mim][BF$_4$] and [C$_4$mim][PF$_6$] As a Function of Temperature T

	C_P/J·mol^{-1}·K^{-1}	
T/K	[C$_4$mim][BF$_4$]	[C$_4$mim][PF$_6$]
308.16	367.26	410.64
313.16	367.64	413.48
318.16	370.39	417.74
323.16	371.89	422.01
328.22	373.73	423.43
333.22	375.92	426.27
338.19	377.15	429.11
343.18	380.16	433.37
348.25	382.69	436.22
353.18	384.80	439.06
358.25	386.99	441.90
363.18	389.18	443.32
368.17	390.00	444.74
373.21	390.04	447.58
378.20	392.18	450.43
383.17	393.64	454.69
388.20	395.28	457.53
393.17	396.49	460.37
398.20	397.93	463.21
403.20	400.74	468.90
408.16	403.88	470.32
413.19	403.49	471.74
418.19	404.98	473.16
423.22	406.62	474.58

3.3. Thermal Conductivity of IoNanofluids. The thermal conductivity of the IoNanofluids produced by adding MWCNTs to [C$_6$mim][BF$_4$], [C$_4$mim][PF$_6$], [C$_6$mim][PF$_6$], [C$_4$mim][CF$_3$SO$_3$], and [C$_4$mpyrr][(CF$_3$SO$_2$)$_2$N] were also measured at temperatures between 293 and 353 K, at a pressure of 0.1 MPa. Results for the IoNanofluids from [C$_2$mim][(CF$_3$SO$_2$)$_2$N], [C$_4$mim][(CF$_3$SO$_2$)$_2$N], [C$_6$mim][(CF$_3$SO$_2$)$_2$N], [C$_8$mim][(CF$_3$SO$_2$)$_2$N] and [C$_4$mim][BF$_4$] have been reported in ref 6. Figure 6 and Table 8 show the results obtained for these new fluids. It can be seen that the variation is linear with temperature, as found for the pure ionic liquids, and that no data point departs from linearity by more than ± 0.25 % (see Figure 7). Table 5 also shows the coefficients of regression for eq 2 and the root-mean-square deviations of the fits.

Figure 8 shows the thermal conductivity enhancement as a function of temperature for the IoNanofluids studied. Some of the fluids show a temperature dependent enhancement ([C$_6$mim][BF$_4$] and [C$_4$mim][CF$_3$SO$_3$]), while the remaining compounds demonstrate a constant increase (5 % for [C$_4$mpyrr][(CF$_3$SO$_2$)$_2$N], 3.4 % for [C$_4$mim][PF$_6$], and 1.8 % for [C$_6$mim][PF$_6$]). This result is similar to the behavior found previously for other nanofluids.[1] In general IoNanofluids containing [PF$_6$]$^-$ based ionic liquids have the smallest enhancement in thermal conductivity while those based on [C$_6$mim][BF$_4$] had the largest (9 % on average) change. No smooth dependence on the cations or anion was found, which is in agreement with the results obtained for the [C$_n$mim]$^+$ based ionic liquids presented in ref 6.

The interpretation of the thermal conductivity enhancement in nanofluids has been the object of many publications, since the pioneering work of Maxwell.[36] This model was developed for millimeter and micrometer-sized particles suspended in liquids, and the ratio between the thermal conductivity of the nanofluid and that of the base fluid, $\lambda_{NF}/\lambda_{BF}$, was found to depend on the thermal conductivity of both phases (solid and liquid) and on the volume fraction of the solid. The model, adapted for the IoNanofluids, is shown in eq 4

$$\frac{\lambda_{NF}}{\lambda_{IL}} = \frac{\lambda_{CNT} + 2\lambda_{IL} + 2\varphi_{CNT}(\lambda_{CNT} - \lambda_{IL})}{\lambda_{CNT} + 2\lambda_{IL} - \varphi_{CNT}(\lambda_{CNT} - \lambda_{IL})} \quad (4)$$

where λ_{NF}, λ_{IL}, λ_{CNT} are, respectively, the thermal conductivity of the nanofluid, of the ionic liquid, and of the particles (CNT). ϕ_{CNT} is the CNT volume fraction. Extensions of this model to incorporate the shape of the particles, namely cylinders, and the interaction between the particles were developed by Hamilton and Crosser[37] and Hui et al.[38] However, these classical models cannot predict the anomalously high enhancements accurately.[1] Several mechanisms have been proposed, to date, to explain this phenomena. Keblinsky et al.[39] systematized the four different mechanisms for heat transfer that could explain these enhancements, namely (i) Brownian motion of the nanoparticles (ii) liquid layering at the liquid/particle interphase, (iii) the nature of the heat transport in the nanoparticles, and (iv) the effect of nanoparticle clustering. From the analysis of the discussion performed in ref 1 and other publications cited, therein, it is our belief that the effect of the particle surface chemistry and the structure of the interphase particle/fluid are the major mechanisms responsible for the unexpected enhancement in nanofluids.

Table 7. Coefficients of Equation 3

ionic liquid	$b_1 \pm \sigma_{b1}$ / J·mol^{-1}·K^{-1}	$b_2 \pm \sigma_{b2}$ / J·mol^{-1}·K^{-2}	10^4 ($b_3 \pm \sigma_{b3}$) / J·mol^{-1}·K^{-3}	σ / J·mol^{-1}·K^{-1}
[C$_4$mim][BF$_4$]	177.989 ± 23.134	0.80054 ± 0.12732	−6.1596 ± 1.7393	0.9140
[C$_4$mim][PF$_6$]	182.288 ± 32.828	0.87307 ± 0.18067	−4.2115 ± 2.4681	1.2933

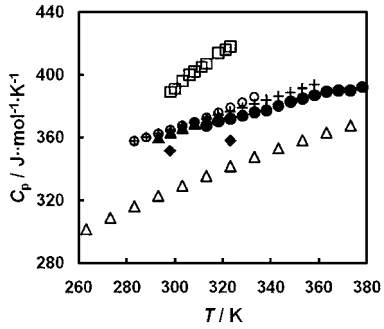

Figure 3. Heat capacity C_P of [C_4mim][BF_4] as a function of temperature T. Data from other authors are also shown. ●, Present work; ○, Rebelo et al.;[26] □, Kim et al.;[27] ◆, Fredlake et al.;[28] +, Waliszewski et al.;[29] △, Van Valkenburg et al.;[30] ∗, Garcia-Miaja et al.;[31] ▲, Garcia-Miaja et al.[32]

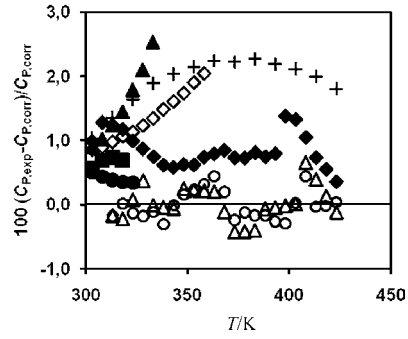

Figure 4. Deviations of the heat capacity C_P reported in this work along with values from others workers as deviations from eq 3, as a function of temperature T. ○, [C_4mim][BF_4], △, [C_4mim][PF_6], present work; ▲, [C_4mim][BF_4], Rebelo et al.;[26] ◇, [C_4mim][BF_4], Waliszewski et al.;[29] +, [C_4mim][BF_4], Van Valkenburg et al.,[30] [C_4mim][BF_4], Garcia-Miaja et al.;[32] ◆, [C_4mim][PF_6], Kabo et al.;[34] ●, [C_4mim][PF_6], Troncoso et al.[35] Results with deviations greater than ± 2 % are not included.

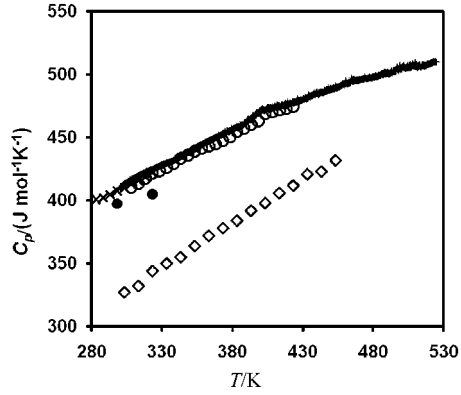

Figure 5. Heat capacity C_P of [C_4mim][PF_6] as a function of temperature T. ○, Present work; ◇, Holbrey et al.;[33] +, Kabo et al.;[34] ●, Fredlake et al.;[28] ×, Troncoso et al.[35]

In order to test these ideas, the heat transfer equation for spherical and infinitely long cylinders has been solved following the model developed by Leong et al.[40,41] This considered the fact that the thermophysical properties of the interfacial layer are different from those of the bulk liquid and of the solid particles. In addition, the interface was used as an additional heat transfer resistance within the description. Equations 5 and 6 were obtained for the thermal conductivity of a nanofluid containing cylindrical particles (our CNTs). (A small difference to eq 7 in ref 43 was found in order to obtain the limiting values of Maxwell model, given by eq 4.

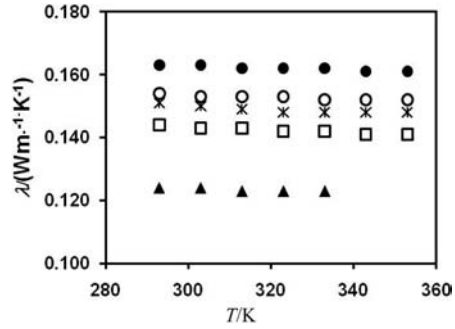

Figure 6. Thermal conductivity λ of IoNanofluids as a function of temperature T with a mass fraction of 0.01 of MWCNT. ●, [C_6mim][BF_4] + MWCNT; ○, [C_4mim][CF_3SO_3] + MWCNT; ▲, [C_4mpyrr][$(CF_3SO_2)_2$N] + MWCNT; ∗, [C_4mim][PF_6] + MWCNT; □, [C_6mim][PF_6] + MWCNT.

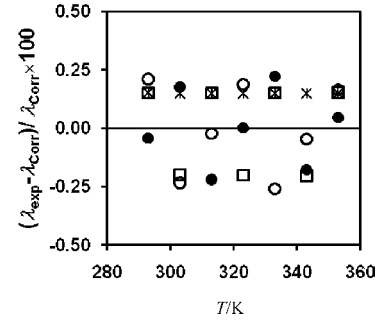

Figure 7. Deviations of the measured thermal conductivity λ from the smoothing eq 2, as a function of temperature T, with mass fraction of 0.01 of MWCNT. ●, [C_6mim][BF_4] + MWCNT; ○, [C_4mim][CF_3SO_3] + MWCNT; ▲, [C_4mpyrr][$(CF_3SO_2)_2$N] + MWCNT; ∗, [C_4mim][PF_6] + MWCNT; □, [C_6mim][PF_6] + MWCNT.

Table 8. Thermal Conductivity λ of IoNanofluids with Mass Fraction of 0.01 of Baytubes As a Function of Temperature T

	λ/W·m^{-1}·K^{-1}				
T/K	[C_6mim][BF_4]/MWCNT	[C_4mim][CF_3SO_3]/MWCNT	[C_4mpyrr][$(CF_3SO_2)_2$N]/MWCNT	[C_4mim][PF_6]/MWCNT	[C_6mim][PF_6]/MWCNT
293	0.158	0.142	0.118	0.145	0.142
303	0.157	0.141	0.118	0.145	0.141
313	0.156	0.140	0.118	0.145	0.141
323	0.155	0.139	0.117	0.144	0.139
333	0.153	0.139	0.117	0.143	0.139
343	0.152	0.138		0.143	0.138
353	0.151	0.138		0.143	0.138

These changes do not affect the overall results and are only introduced here to make the two models consistent with each other.)

$$\lambda_{NF} = \frac{(\lambda_{CNT} - \lambda_{Int})\phi_{CNT}\lambda_{Int}[2\gamma_1^2 - \gamma^2 + 1] + (\lambda_{CNT} + 2\lambda_{Int})\gamma_1^2[\varphi_{CNT}\gamma^2(\lambda_{Int} - \lambda_{LI}) + \lambda_{LI}]}{\gamma_1^2(\lambda_{CNT} + 2\lambda_{Int}) - (\lambda_{CNT} - \lambda_{Int})\varphi_{CNT}[\gamma_1^2 + \gamma^2 - 1]} \quad (5)$$

where

$$\gamma = 1 + \frac{h}{a} \qquad \gamma_1 = 1 + \frac{2h}{a} \quad (6)$$

In these equations, λ_{Int} is the thermal conductivity of the interphase, a is the radius of the cylinder and h the thickness of the interfacial layer (nanolayer at the CNT-IL interface). It

Table 9. Thermal Conductivity Enhancement in the IoNanofluids Studied ($T = 293$ K)

ionic liquid	ρ / kg·m^{-3}	λ_{IL} / W·m^{-1}·K^{-1}	w_{CNT}	ϕ_{CNT}	$\lambda_{NF}/\lambda_{IL} - 1$ experimental	eq 4	eq 5
[C_6mim][BF_4]	1148	0.158	0.01	0.0590	0.048	1.19	1.19
[C_4mim][CF_3SO_3]	1306	0.142	0.01	0.0666	0.094	1.21	1.22
[C_4mpyrr][$(CF_3SO_2)_2$N]	1454	0.118	0.01	0.0735	0.049	1.24	1.25
[C_4mim][PF_6]	1372	0.145	0.01	0.0697	0.034	1.22	1.23
[C_6mim][PF_6]	1298	0.142	0.01	0.0662	0.018	1.21	1.22

should be noted that there is no exact theoretical model to determine h; however, Murshed et al.[41] reported that this parameter is not critical and, therefore, we have assumed in the present calculations that $h \approx 2$ nm.[42] In addition, as no values of λ_{Int} exist for IL/CNT systems, we have used λ_{Int} as an adjustable parameter, keeping in mind that it will be, in principle, intermediate between the values of λ_{IL} and λ_{CNT} (Murshed et al. found $\lambda_{Int} = 60\ \lambda_{IL}$ for ethylene glycol/CNT).

Table 9 shows the results obtained for the five IoNanofluids studied, comparing the experimental enhancement obtained, $\lambda_{NF}/\lambda_{IL} - 1$, with the values found from Maxwell model[36] and Leong et al. model.[40] An average value of $a = 7.5$ nm was used for the MWCNTs and a value of $\lambda_{CNT} = 2000$ W·m^{-1}·K^{-1} was assumed,[42] as no other information regarding the value for the Baytubes exists. Calculations were performed for 293 K, as the temperature dependence of the thermal conductivity of both the ionic liquids and the IoNanofluids is small. Values for the density of the ionic liquids were obtained from the ILThermo database.[43] The limiting value of Maxwell model for volume fractions that oscillate between 0.6 and 0.7 is approximately 1.2, depending also slightly of the thermal conductivity of the ionic liquid. As eq 4 is the limiting value of eq 5, on applying eq 5 to these systems values of $\lambda_{Int} = 0$, and $h = 0$ were obtained, and it predicts a value of the thermal conductivity enhancement greater than found for all the systems studied. The values of Leong et al. model displayed in Table 8 were obtained for $\lambda_{Int} = \lambda_{IL}$, a fact that seems to support that the interphase does not play a very important role in the heat transfer process in these systems, at least for these small volume fractions. Only for systems where the enhancement is of the order of 20 % or greater can the theory describe the effect of the thermal conductivity of the interface solid/liquid, as found for [C_4mim][$(CF_3SO_2)_2$N].[6]

In terms of volume, for such volume fractions, we have occupancy of 6 % of the nanotubes. This might suggest that the IoNanofluids consist the same type of nanostructural organization found by Lopes and Padua,[44] using molecular dynamics simulations for [$C_n$mim][$(CF_3SO_2)_2$N] and [$C_n$mim][PF_6] ionic liquids. They found that for ionic liquids with alkyl chains where $n \geq 4$, aggregation of the alkyl chains into nonpolar domains is observed. This creates a tridimensional network of ionic channels formed by the anions and the Imidazolium rings of the cations and provides evidence of microphase separation between polar and nonpolar domains within the liquid phase structure. The CNTs when dispersed in the ionic liquid are likely to interact preferentially with the nonpolar domains associated with the alkyl chains, therefore, creating microclusters that will enhance the heat transfer. However, as the size of the nanotubes, not accounted for in Leong et al. model, is significant (1 to 10) μm, the structure of the IoNanofluids is likely to be different compared with that of the base fluid. This will be analyzed in the future. Results obtained for the heat capacity of these systems, described in the following section, will also contribute to the discussion about the structure of these systems and their influence on heat transfer and storage.

Table 10. Heat Capacity C_P of [C_4mim][PF_6] IoNanofluid for Mass Fractions of 0.01 and 0.015 of Baytubes as a Function of Temperature T

T/K	C_P/J·mol^{-1}·K^{-1} 1 wt %	1.5 wt %
308.16	1.46	1.48
313.16	1.48	1.49
318.16	1.50	1.50
323.16	1.50	1.50
328.22	1.51	1.50
333.22	1.52	1.50
338.19	1.52	1.52
343.18	1.55	1.55
348.25	1.61	1.59
353.18	1.67	1.63
358.25	1.67	1.65
363.18	1.66	1.65
368.17	1.64	1.64
373.21	1.64	1.63
378.20	1.63	1.63
383.17	1.62	1.64
388.20	1.62	1.63
393.17	1.62	1.64
398.20	1.62	1.65
403.20	1.63	1.66
408.16	1.63	1.67
413.19	1.64	1.68
418.19	1.64	1.68
423.22	1.65	1.68

3.4. Heat Capacity of an IoNanofluid. The heat capacity of an IoNanofluid was measured and the results for [C_4mim][PF_6] + mass fraction of 0.01 and 0.015 Baytubes are shown in Table 10 and Figure 9. The results are very surprising, as a large maximum in the heat capacity as a function of temperature is also found compared with the bulk ionic liquid. Similar data has not been reported previously for nanofluids. Figure 10 shows the heat capacity enhancement, $C_{P,NF}/C_{P,IL} - 1$, as a function of temperature, where the values for the pure ionic liquid were obtained from eq 3 and Table 7. The maximum observed, shaped as a dome as in critical behavior in pure fluids and near immiscibility critical end points,[45] is clear and shows a peak of

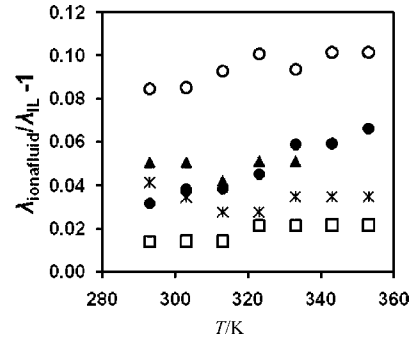

Figure 8. Thermal conductivity λ enhancement in the IonNanofluids with mass fraction of 0.01 of MWCNT as a function of temperature T. ●, [C_6mim][BF_4] + MWCNT; ○, [C_4mim][CF_3SO_3] + MWCNT; ▲, [C_4mpyrr][$(CF_3SO_2)_2$N] + MWCNT; ∗, [C_4mim][PF_6] + MWCNT; □, [C_6mim][PF_6] + MWCNT.

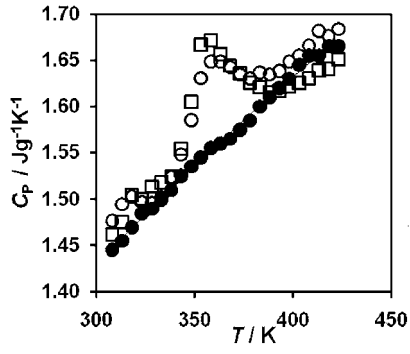

Figure 9. Heat capacity C_P of [C_4mim][PF_6] IoNanoFluid for two different MWCNT mass fractions of 0.01 and 0.015 as a function of temperature *T*. ●, [C_4mim][PF_6]; □, [C_4mim][PF_6] + MWCNT (1 wt %); ○, [C_4mim][PF_6] + MWCNT (1.5 wt %).

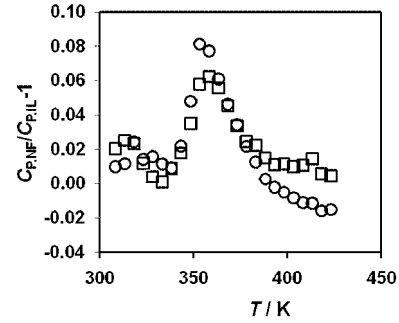

Figure 10. Heat capacity C_P enhancement of [C_4mim][PF_6] IoNanofluid for two different MWCNT mass fractions of 0.01 and 0.015 as a function of temperature *T*. □, [C_4mim][PF_6] + MWCNT with mass fraction of 0.01; ○, [C_4mim][PF_6] + MWCNT with mass fraction of 0.01.

8 % compared with the bulk liquid irrespective of the CNT loading. Some noise within the accuracy of the measurements is found the lower and higher temperatures. Further investigations using other ionic liquids and the application of phenomenological theories of criticality will be performed in order to understand the interactions involved in these systems and to examine whether the aggregation phenomena/nanostructural organization is present and is important in the mechanism of the effects observed.

4. Conclusions

Thermal conductivity and heat capacity of ionic liquids and IoNanofluids with MWCNTs have been measured as a function of temperature. The thermal conductivity data obtained have an uncertainty of (3 to 5) % and, where available, is in good agreement with previously reported data. The data for the heat capacity also agrees well with published data and has an estimated uncertainty of 1 %.

In the case of IoNanofluids, the data is completely new and cannot be compared with other data. Moderate thermal conductivity enhancements between (2 and 9) % were found for the systems studied, showing a weak dependence on temperature. For heat capacity, an enhancement of up to 8 % was found for C_4mim][PF_6] with both 0.01 and 0.015 Baytubes, a phenomena found for the first time for nanofluids. The behavior of these nanofluids, along with the specific behavior of ionic liquids of the type studied, suggests the existence of nanocluster formation and preferred paths for heat transfer and storage, a fact that will be the subject of further studies.

Acknowledgment

The authors would like to thank Bayer Material Science for supplying the Baytubes, FCT - Fundação para a Ciência e para a Tecnologia, Portugal for Pluriannual funding of CCMM. A.P.C.R. thanks FCT for Ph.D. Grant SFRH/BD/39940/2007 and E.L. for postdoctoral Grant SFRH/BPD/42035/2007. This work also was supported by an EU Marie Curie Early Stage Training Site Fellowship, contract number HPMT-GH-00-00147-03, QUILL, and a Portfolio Partnership grant from the EPSRC.

Literature Cited

(1) Murshed, S.; Leong, K.; Yang, C. Thermophysical and electrokinetic properties of nanofluids - A critical review. *Appl. Therm. Eng.* **2008**, *28* (17−18), 2109–2125.
(2) Choi, S. U. S.; Zhang, Z. G.; Keblinski, P. Enhancing thermal conductivity of fluids with nanoparticles. In *Developments and Applications of Non-Newtonian Flows*; Siginer, D. A., Wang, H. P., Eds.; ASME: New York, 1995; Vol. FED-Vol. 231/MD-Vol. *66*, pp 99−105.
(3) Das, S.; Choi, S.; Patel, H. Heat transfer in Nanofluids - A review. *Heat Transfer Eng.* **2006**, *27* (10), 3–19.
(4) Keblinski, P.; Prasher, R.; Eapen, J. Thermal conductance of nanofluids: is the controversy over. *J. Nanopart. Res.* **2008**, *10* (7), 1089–1097.
(5) Das, S. Nanofluids - The cooling medium of the future. *Heat Transfer Eng.* **2006**, *27* (10), 1–2.
(6) Ribeiro, A. P. C.; Goodrich, P.; Hardacre, C.; Lourenço, M. J. V.; Nieto de Castro, C. A. Thermal conductivity of ionic liquids with carbon nanotubes (IoNanofluids). *Green Chem.* **2009**, submitted.
(7) Earle, M.; Seddon, K. Ionic liquids. Green solvents for the future. *Pure Appl. Chem.* **2000**, *72* (7), 1391–1398.
(8) Nunes, V. M. B.; Lourenço, M. J. V.; Santos, F. J. V.; Matos Lopes, M. L. S.; Nieto de Castro, C. A. Accurate Measurements of Physico-Chemical Properties on Ionic Liquids and Molten Salts. In *Ionic Liquids and Molten Salts: Never the Twain*; Seddon, K. R., Gaune-Escard, M., Eds.; John Wiley: New York, 2010; pp 229−263.
(9) Wasserscheid, P.; Welton, T. *Ionic Liquids in Synthesis*; Wiley-VCH: Weinheim, 2007.
(10) Holbrey, J. Heat capacities of common ionic liquids - Potential applications as thermal fluids. *Chim. Oggi* **2007**, *25* (6), 24–26.
(11) Franca, J.; de Castro, C.; Lopes, M.; Nunes, V. Influence of Thermophysical Properties of Ionic Liquids in Chemical Process Design. *J. Chem. Eng. Data* **2009**, *54* (9), 2569–2575.
(12) Fukushima, T.; Kosaka, A.; Ishimura, Y.; Yamamoto, T.; Takigawa, T.; Ishii, N.; Aida, T. Molecular ordering of organic molten salts triggered by single-walled carbon nanotubes. *Science* **2003**, *300* (5628), 2072–2074.
(13) Fukushima, T.; Aida, T. Ionic liquids for soft functional materials with carbon nanotubes. *Chem.—Eur. J.* **2007**, *13* (18), 5048–5058.
(14) Bonhote, P.; Dias, A.; Papageorgiou, N.; Kalyanasundaram, K.; Gratzel, M. Hydrophobic, highly conductive ambient-temperature molten salts. *Inorg. Chem.* **1996**, *35* (5), 1168–1178.
(15) Holbrey, J.; Seddon, K.; Wareing, R. A simple colorimetric method for the quality control of 1-alkyl-3-methylimidazolium ionic liquid precursors. *Green Chem.* **2001**, *3* (1), 33–36.
(16) Villagran, C.; Deetlefs, M.; Pitner, W.; Hardacre, C. Quantification of halide in ionic liquids using ion chromatography. *Anal. Chem.* **2004**, *76* (7), 2118–2123.
(17) Ramires, M. L. V.; Decastro, C. A. N.; Fareleira, J.; Wakeham, W. A. Thermal-Conductivity of Aqueous Sodium-Chloride Solutions. *J. Chem. Eng. Data* **1994**, *39* (1), 186–190.
(18) Chen, H.; He, Y.; Zhu, J.; Alias, H.; Ding, Y.; Nancarrow, P.; Hardacre, C.; Rooney, D.; Tan, C. Rheological and heat transfer behaviour of the ionic liquid, [C(4)mim][NTf2]. *Int. J. Heat. Fluid Flow* **2008**, *29* (1), 149–155.
(19) Carslaw, H. S.; Jaeger, J. C. *Conduction of Heat in Solids*; Oxford University Press: London, 1959; p 25.
(20) Kluitenberg, G.; Ham, J.; Bristow, K. Error Analysis Of The Heat Pulse Method For Measuring Soil Volumetric Heat-Capacity. *Soil Sci. Soc. Am. J.* **1993**, *57* (6), 1444–1451.
(21) Ge, R.; Hardacre, C.; Nancarrow, P.; Rooney, D.; Thermal conductivities of ionic liquids over the temperature range from 293 K to 353, K. *J. Chem. Eng. Data* **2007**, *52* (5), 1819–1823.
(22) de Castro, C. A. N.; Lourenco, M. J. V.; Sampaio, M. O. Calibration of a DSC: its importance for the traceability and uncertainty of thermal measurements. *Thermochim. Acta* **2000**, *347*, 85–91.
(23) Lourenco, M. J. V.; Santos, F. J. V.; Ramires, M. L. V.; de Castro, C. A. N. Isobaric specific heat capacity of water and aqueous cesium chloride solutions for temperatures between 298 and 370 K at p = 0.1 MPa. *J. Chem. Thermodyn.* **2006**, *38* (8), 970–974.
(24) Sampaio, M. O.; de Castro, C. A. N. Heat capacity of liquid terpenes. *Fluid Phase Equilib.* **1998**, *150−151*, 789–796.
(25) Tomida, D.; Kenmochi, S.; Tsukada, T.; Qiao, K.; Yokoyama, C. Thermal Conductivities of [bmim][PF6], [hmim][PF6], and [omim][PF6]

from 294 to 335 K at Pressures up to 20 MPa. *Int. J. Thermophys.* **2007**, *28* (4), 1147–1160.
(26) Rebelo, L.; Najdanovic-Visak, V.; Visak, Z.; da Ponte, M.; Szydlowski, J.; Cerdeirina, C.; Troncoso, J.; Romani, L.; Esperanca, J.; Guedes, H.; de Sousa, H. A detailed thermodynamic analysis of [C(4)mim][BF4] plus water as a case study to model ionic liquid aqueous solutions. *Green Chem.* **2004**, *6* (8), 369–381.
(27) Kim, K.; Shin, B.; Lee, H.; Ziegler, F. Refractive index and heat capacity of 1-butyl-3-methylimidazolium bromide and 1-butyl-3-methylimidazolium tetrafluoroborate, and vapor pressure of binary systems for 1-butyl-3-methylimidazolium bromide plus trifluoroethanol and 1-butyl-3-methylimidazolium tetrafluoroborate plus trifluoroethanol. *Fluid Phase Equilib.* **2004**, *218* (2), 215–220.
(28) Fredlake, C.; Crosthwaite, J.; Hert, D.; Aki, S.; Brennecke, J. Thermophysical properties of imidazolium-based ionic liquids. *J. Chem. Eng. Data* **2004**, *49* (4), 954–964.
(29) Waliszewski, D.; Stepniak, I.; Piekarski, H.; Lewandowski, A. Heat capacities of ionic liquids and their heats of solution in molecular liquids. *Thermochim. Acta* **2005**, *433* (1−2), 149–152.
(30) Van Valkenburg, M.; Vaughn, R.; Williams, M.; Wilkes, J. Thermochemistry of ionic liquid heat-transfer fluids. *Thermochim. Acta* **2005**, *425* (1−2), 181–188.
(31) Garcia-Miaja, G.; Troncoso, J.; Romani, L. Excess properties for binary systems ionic liquid plus ethanol: Experimental results and theoretical description using the ERAS model. *Fluid Phase Equilib.* **2008**, *274* (1−2), 59–67.
(32) Garcia-Miaja, G.; Troncoso, J.; Romani, L. Excess molar properties for binary systems of alkylimidazolium-based ionic liquids plus nitromethane. Experimental results and ERAS-model calculations. *J. Chem. Thermodyn.* **2009**, *41* (3), 334–341.
(33) Holbrey, J.; Reichert, W.; Reddy, R.; Rogers, R. Heat capacities of ionic liquids and their applications as thermal fluids. In *Ionic Liquids as Green Solvents: Progress and Prospects*; Rogers, R. D., Seddon, K. R., Eds.; ACS Symposium Series 856; American Chemical Society: Washington, DC, 2003; pp 121−133.
(34) Kabo, G.; Blokhin, A.; Paulechka, Y.; Kabo, A.; Shymanovich, M.; Magee, J. Thermodynamic properties of 1-butyl-3-methylimidazolium hexafluorophosphate in the condensed state. *J. Chem. Eng. Data* **2004**, *49* (3), 453–461.
(35) Troncoso, J.; Cerdeirina, C.; Sanmamed, Y.; Romani, L.; Rebelo, L. Thermodynamic properties of imidazolium-based ionic liquids: Densities, heat capacities, and enthalpies of fusion of [bmim][PF6] and [bmim][NTf2]. *J. Chem. Eng. Data* **2006**, *51* (5), 1856–1859.
(36) Maxwell, J. C. *A Treatise on Electricity and Magnetism*, 3rd ed.; Clarendon Press: Oxford, UK, 1891.
(37) Hamilton, R.; Crosser, O. Thermal Conductivity of Heterogeneous 2-Component Systems. *Ind. Eng. Chem. Fundam.* **1962**, *1* (3), 187.
(38) Hui, P.; Zhang, X.; Markworth, A.; Stroud, D. Thermal conductivity of graded composites: Numerical simulations and an effective medium approximation. *J. Mater. Sci.* **1999**, *34* (22), 5497–5503.
(39) Keblinski, P.; Phillpot, S.; Choi, S.; Eastman, J. Mechanisms of heat flow in suspensions of nano-sized particles (nanofluids). *Int. J. Heat Mass Transfer* **2002**, *45* (4), 855–863.
(40) Leong, K.; Yang, C.; Murshed, S. A model for the thermal conductivity of nanofluids - the effect of interfacial layer. *J. Nanopart. Res.* **2006**, *8* (2), 245–254.
(41) Murshed, S.; Leong, K.; Yang, C. Investigations of thermal conductivity and viscosity of nanofluids. *Int. J. Therm. Sci.* **2008**, *47* (5), 560–568.
(42) Choi, S.; Zhang, Z.; Yu, W.; Lockwood, F.; Grulke, E. Anomalous thermal conductivity enhancement in nanotube suspensions. *Appl. Phys. Lett.* **2001**, *79* (14), 2252–2254.
(43) Ionic Liquids Database - (IL Thermo). NIST Standard Reference Database No. 147. NIST, U.S. Secretary of Commerce: Washington, DC, 2006.
(44) Lopes, J.; Padua, A. Nanostructural organization in ionic liquids. *J. Phys. Chem. B* **2006**, *110* (7), 3330–3335.
(45) Troncoso, J.; Peleteiro, J.; Mendez-Castro, P.; Romani, L. Critical behavior of the heat capacity for binary mixtures of room temperature ionic liquids and molecular solvents. In *1st Iberian Meeting on Ionic Liquids*; Coutinho, J. A. P., Ed.; Sociedade Portuguesa de Química: Aveiro, Portugal, 2009; p 175.
(46) Sabbah, R.; An, X.; Chickos, J.; Leitao, M.; Roux, M.; Torres, L. Reference materials for calorimetry and differential thermal analysis. *Thermochim. Acta* **1999**, *331* (2), 93–204.
(47) Preston-Thomas, H. The international temperature scale of 1990 (ITS-90). BIPM. *Metrologia* **1990**, *27*, 3–10.
(48) Malcolm, W., Chase, J., Eds.; NIST-JANAF Thermochemical Tables, 4th ed. *J. Phys. Chem. Ref. Data* **1998**, (Monograph 9).

Received for review July 31, 2009. Accepted October 12, 2009.

JE900648P